Earthquake Research Advances 5 (2025) 100395

Contents lists available at ScienceDirect

Earthquake Research Advances

journal homepage: www.keaipublishing.com/en/journals/earthquake-research-advances

Recorded responses of Four Tall buildings in South China to the *M* 7.9 Myanmar Earthquake on March 28, 2025

Tao Fan [a,b,c], Zhe Qu [a,b,*], Jiang Yang [c,d,e], Juan Qin [f], Xiaofeng Xu [g], Yuxiu Chen [c,d,e], Qiong Yuan [d,e]

[a] *Key Laboratory of Earthquake Engineering and Engineering Vibration, Institute of Engineering Mechanics, China Earthquake Administration, Harbin, 150080, China*
[b] *Key Laboratory of Earthquake Disaster Mitigation, Ministry of Emergency Management, Harbin, 150080, China*
[c] *Hubei Key Laboratory of Earthquake Early Warning, Hubei Earthquake Agency, Wuhan, 430071, China*
[d] *Wuhan Institute of Seismologic Instruments Co., Ltd., Xianning, 437100, China*
[e] *Engineering Technology Research Center for Earthquake Monitoring and Early Warning Disposal of Major Projects in Hubei Province, Xianning, 437100, China*
[f] *Chongqing Earthquake Agency, Chongqing, 401147, China*
[g] *Hainan Earthquake Agency, Haikou, 570203, China*

ARTICLE INFO

Keywords:
Myanmar earthquake
High-rise buildings
Long-period ground motion
Far-field earthquakes
Seismic structural monitoring

ABSTRACT

This paper reports the recorded structural responses of four 170 m–320 m tall buildings in China to the mainshock of the *M* 7.9 Myanmar earthquake on March 28, 2025. The buildings are located approximately 1 200 km–2 000 km away from the epicenter. The following observations are made by preliminary analysis of the data: (1) the base motion of the buildings exhibited significant long-period components in the range of 2 s–10 s; (2) the identified fundamental periods were much larger than the empirical equations in the design codes, suggesting that the empirical equations may be overly conservative; (3) the amplification of floor accelerations was much more significant than code provisions for determining the seismic demands on non-structural elements, possibly attributing to the overly high damping ratios assumed in the design codes; (4) the buildings exhibited large enough equivalent lateral stiffnesses to satisfy the drift limit under frequent earthquakes by the Chinese seismic provisions, and (5) the significant durations of the shaking of the upper floors of the buildings were comparable to those of the base motions.

1. Introduction

On March 28, 2025, a *M* 7.9 earthquake with a focal depth of 30 km struck central Myanmar (Cai et al., 2025). According to the U.S Geological Survey (2025), the maximum intensity could have reached X (Extreme) on the modified Mercalli scale, constituting Myanmar's most significant earthquake since 1912. The epicenter was only 17 km away from Mandalay, the nation's second-largest city. The earthquake resulted in extensive destruction throughout Myanmar and considerable damage in neighboring countries. It directly claimed approximately 5 352 lives in Myanmar alone (Mizzima, 2025), making it the second most deadly earthquake in the country's modern history, surpassed by the 1930 Bago earthquake (The Washington Post, 2025). It also stands as the deadliest earthquake globally since the 2023 Türkiye-Syria earthquakes.

In addition to the great impact on Myanmar, the earthquake claimed another 93 lives in Bangkok, Thailand, which was approximately 1 000 km away from the epicenter. Among them, 88 deaths were caused by the complete collapse of the 33-story State Audit Office building, which was already topped-out but still under construction when the earthquake occurred (https://en.wikipedia.org/wiki/2025_Myanmar_earthquake). Although the specific causes of the extraordinary collapse were still under investigation by a government-appointed committee (Pimanmas,

* Corresponding author. Key Laboratory of Earthquake Engineering and Engineering Vibration, Institute of Engineering Mechanics, China Earthquake Administration, Harbin, 150080, China.
E-mail address: quz@iem.ac.cn (Z. Qu).

Production and Hosting by Elsevier on behalf of KeAi

https://doi.org/10.1016/j.eqrea.2025.100395
Received 10 May 2025; Received in revised form 18 May 2025; Accepted 19 May 2025

2025), it reminds people of the amplified effects of distant earthquakes on tall buildings, especially if they are on soft soil, which has been repeatedly observed during historical earthquakes. For example, the 1985 *M* 8.1 Mexico City earthquake caused severe damage to numerous mid- and high-rise buildings approximately 350 km from the epicenter (Meli and Rosenblueth, 1986; Seed et al., 1988). The 2008 *M* 8.0 Wenchuan earthquake in China caused widespread damage to non-structural components and the coupling beams in some high-rise residential buildings of shear wall structures in Baoji, 520 km from the epicenter, and Xi'an, 700 km from the epicenter (Liang et al., 2009). The 2010 *M* 8.8 Chilean earthquake caused substantial damage to the high-rise structures in distant urban centers such as Santiago, despite being approximately 335 km away from the epicenter (Carpenter et al., 2011; Earthquake Engineering Research Institute, 2010). The 2011 *M* 9.0 Tohoku earthquake in Japan led to significant shaking of the many skyscrapers in Shinjuku, Tokyo, approximately 370 km from the epicenter (Takewaki et al., 2011), resulting in damage to the non-structural components in the building and widespread anxiety among people in the buildings during the earthquake (Saito, 2016; Kanda et al., 2021).

Structural monitoring provides invaluable data basis for better understanding seismic behavior and for calibrating the dynamic properties of real-world tall buildings. The structural responses of 20 buildings of 2- to 54-story tall in Los Angeles in the 1997 *M* 6.7 Northridge earthquake in southern California, US, facilitated analysis of the dynamic properties of those structures, which supported the later revision of the structural design specifications (Naeim, 1997). The monitoring systems on some tall buildings in Tokyo provided invaluable data on the strong vibration of the buildings during the 2011 *M* 9.0 Tohoku earthquake to calibrate the numerical models, analysis methods and key parameters of real-world tall buildings (Kasai et al., 2012). The monitoring data of the 492 m-tall Shanghai World Financial Center (SWFC) helped calibrate the seismic design of the tallest building in Shanghai by comparing the first three natural frequencies of the completed building, the shaking table test model, and the numerical model for the design (Shi et al., 2012). The recorded seismic responses of tall residential buildings of over 160 m height in Wuhan during the 2022 *M* 6.9 Hualien earthquake in Taiwan, China, showcased the discrepancy of the estimated fundamental period and assumed overly high damping ratio for the seismic design (Fan et al., 2025).

Despite the many successful structural seismic monitoring systems on tall buildings over the globe, there remains a lack of public real-world data on instrumented tall buildings affected by major earthquakes. In light of the great importance of such data for the advancement of the research and practice of the seismic design of tall buildings, this paper reports the recorded responses of four tall buildings exceeding 160 m in height in south China during the Myanmar earthquake. Followed by a brief introduction to the buildings and their monitoring systems, the remaining of this paper first summarizes the obtained acceleration records on the buildings during the earthquake, describes the characteristics of the recorded motions at the base, featuring their long-period components, and then analyzes the engineering demand parameters, i.e., the peak floor accelerations (*PFA*) and the inter-story drift ratios (*IDR*) of the buildings during the earthquake.

2. Instrumented tall buildings of concern

The four instrumented tall buildings of concern are the Financial City Tower (FCT) in Chengdu, the International Financial City (IFC) in Chongqing, the Jinyin Lake Tower (JLT) in Wuhan, and the CCCC Hainan Base (CHB) headquarter in Sanya. Fig. 1 depicts their appearances and locations with respect to the epicenter of the March 28 Myanmar earthquake. Their epicentral distances range from approximately 1 200 km to 2 100 km. While the FCT in Chengdu was on a site of Intensity 7 [0.1*g* peak ground acceleration (*PGA*) for 10% in 50 yrs design basis earthquakes] as per the Chinese Seismic Code (GB

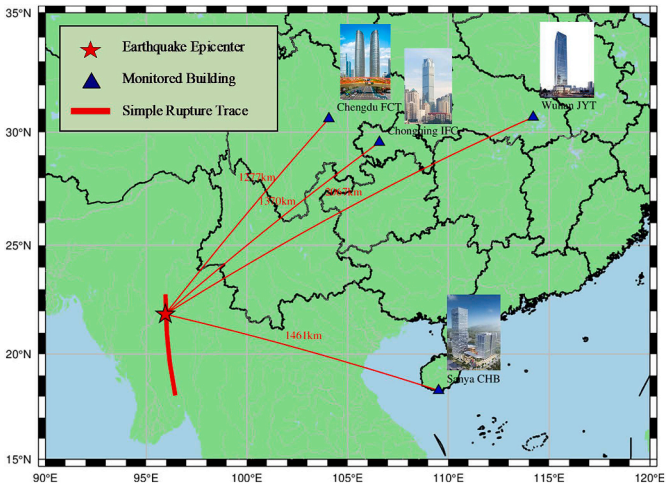

Fig. 1. Map of epicenter and instrumented buildings of concern.

50011-2010, 2016), the other three buildings were in Intensity 6 regions (0.05*g* PGA for design basis earthquakes), which is the lowest allowable seismic design level in China.

Fig. 2 illustrates the elevations and typical floor plans of the buildings. Their heights range from approximately 170 m to 320 m. All four buildings employed a concrete frame-core tube structural system without outrigger or belt trusses. More information on the buildings is summarized in Table 1.

Also denoted in Fig. 2 by the red circles are the locations of instruments in the buildings. At each location was installed a three-component accelerograph along with a separate multiple-channel data log. The different data logs in the same buildings were synchronized by Network Time Protocol (NTP). The Chengdu FCT was equipped with mechanical force-balanced ETNA2 with a dynamic range of more than 130 dB, while the other three buildings used REMOS-VOLCAS seismographs developed by Wuhan Institute of Seismologic Instruments Co., Ltd, which used MEMS capacitive sensors of more than 113 dB dynamic range. All instrument was installed in the extra-low-voltage riser rooms in the core tubes of the buildings. All sensors were aligned with the primary axes of the host buildings, which are denoted as *x*- and *y*-direction for the horizontal channel and the *z*-direction for the vertical channel. More parameters of the sensors are referred to Table 2.

3. Acceleration response records

While the full collection of the obtained acceleration response data is made available as attachments of this paper for the research community, Fig. 3 demonstrates the data in both the time and the frequency domain for selected instrumented floors along the *y*-axis of the buildings. The raw data were baseline corrected and filtered with a 4^{th}-order Butterworth non-causal bandpass filter of 0.1 Hz–20 Hz. The earthquake event can be clearly seen from the acceleration time histories of all the floors of buildings. The peak acceleration was significantly amplified from the base of the buildings to the top. The time-domain responses of the buildings also feature long durations of several minutes.

In the frequency domain, the Fourier spectra clearly show the buildings' fundamental periods. The thus-identified fundamental periods of the buildings along the two orthogonal horizontal axes are listed in the last two columns of Table 1. These results are compared with the empirical equations in building design codes in Chinese and the USA in Fig. 4. The identified periods of the four RC tall buildings are much larger than the estimates by the empirical equations for concrete structures in Eq. (1a) and Eq. (2) recommended by the Chinese load code for building structures (GB 50009-2012, 2012). They are even greater than the estimated periods for steel structures by Eq. (1b) in the same

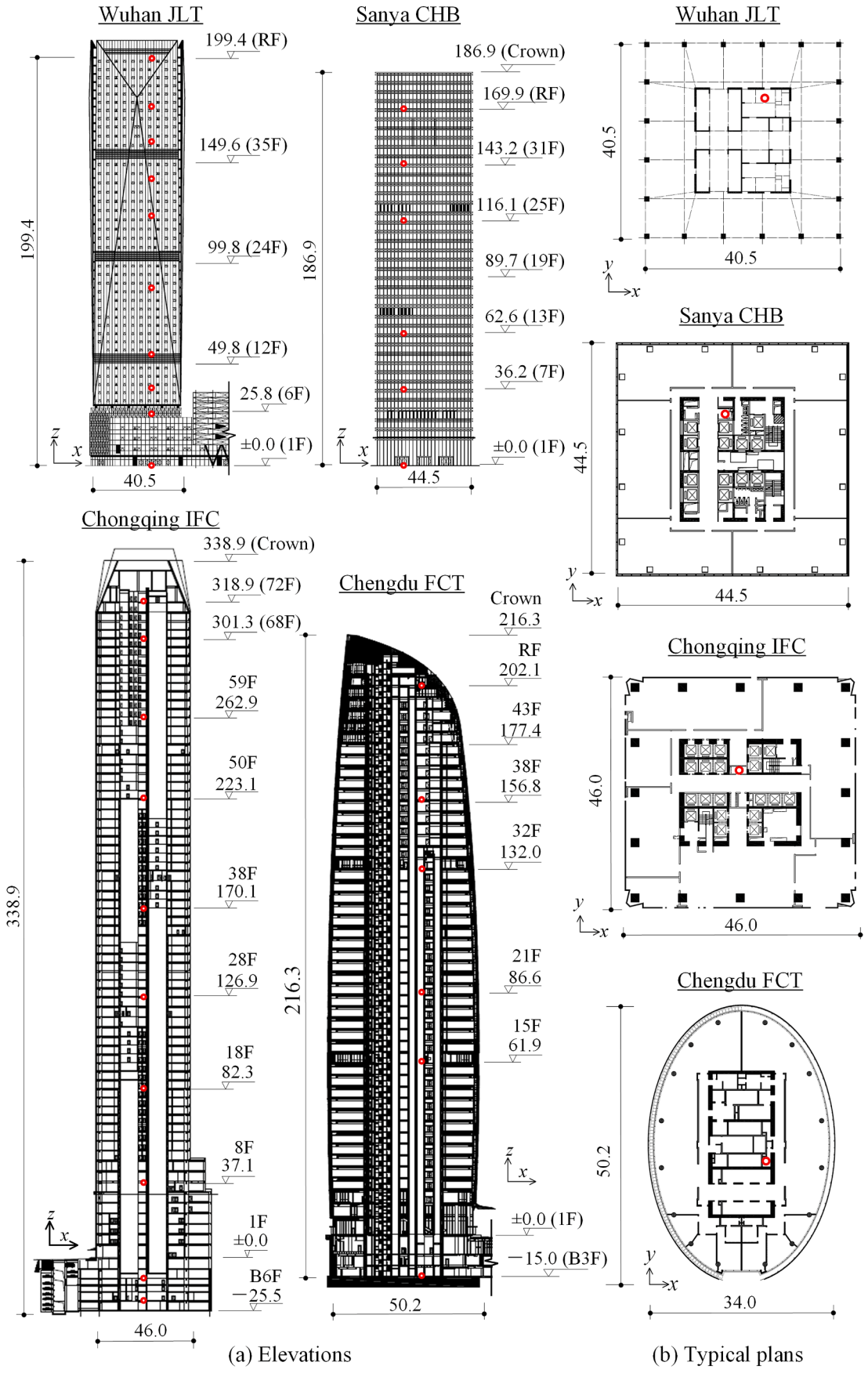

Fig. 2. Location of sensors in (a) elevations, and (b) typical floor plans of buildings (unit: m).

Table 1
Basis information of instrumented tall buildings of concern during the 2025 Myanmar earthquake.

Buildings	Location	Epicenter distance (km)	Design intensity	Site class	Building height H (m)	No. Floors		T_x (s)	T_y (s)
						Above ground	Basement		
Financial City Tower (FCT)	Chengdu	1 277	7	II	202.2	48	3	4.14	3.16
International Financial City (IFC)	Chongqing	1 370	6	I	323.9	72	6	6.18	6.49
Jinyin Lake Tower (JLT)	Wuhan	2 067	6	III	199.4	46	3	4.28	4.15
CCCC Hainan Base (CHB)	Sanya	1 461	6	II	169.9	36	3	2.88	2.71

Table 2
Key parameters of accelerographs.

Device model	Type of sensor	Measurement range	Dynamic range (dB)	Frequency response (Hz)	Linearity error	Transverse sensitivity ratio
REMOS-VOLCAS	MEMS Capacitive	$\pm 2g$	> 113	0.05 Hz–160 Hz	$<0.3\%$	$<1\%$
ETNA2	Mechanical Force Balanced	$\pm 1g$, $\pm 2g$, $\pm 4g$ (optional)	> 130	DC-200 Hz	$<0.1\%$	$<1\%$

code. The empirical equation in the US code [Eq. (3) in ASCE 7–22 (2022)] outperforms the Chinese equations for concrete structures but still underestimates the periods. Linear regression shows that a simple estimate of $T_1 = 0.02H$ best fits the fundamental periods of the four tall buildings during the earthquake.

$$T_1 = 0.007H \text{ for concrete structures} \tag{1a}$$

$$T_1 = 0.013H \text{ for steel structures} \tag{1b}$$

where T_1 is the fundamental period, and H is the total height of the structure.

$$T_1 = 0.53 + 0.08 \times 10^{-2}\frac{H^2}{D} \tag{2}$$

where D is the diameter at mid-height of the structure, and is taken as $D = 40$ m in Fig. 4.

$$T_1 = C_t H^x \tag{3}$$

where C_t and x are structural system-specific coefficients. For the four buildings of concern, $C_t = 0.0488$ and $x = 0.75$ recommended for "all other structures" are adopted.

4. Base motion intensities

The recorded motion at the instrumented floor closest to the ground level of each building is taken as the earthquake excitation imposed on the structure and is referred to as the base motion hereinafter. Although such base motions are commonly assumed to mimic the free-site ground motion, this assumption is subject to certain limitations, such as minimal soil-structure interaction (SSI), shallow foundations, and the absence of base isolation or flexible base components. For the sake of rigor, we refrain from referring to them as ground motions throughout the paper, although they are sometimes compared with the ground motion requirements by the code. Fig. 5 shows the acceleration response spectra S_a of the base motions with 5% viscous damping. The spectra exhibit significant peaks in the long-period range of more than 5 s. Although the fundamental periods of some of the buildings, such as FCT and IFC, come close to the peaks of the spectra of the base motions, it is not the case for JLT and CHB in both directions and FCT in the x-direction. It suggests that the significant long-period components in the base motions were attributed more to the long path of the seismic wave rather than the effect of the building vibration.

Fig. 6 compares the design spectra and the response spectra of the recorded base motion of the buildings, all normalized by their respective peak ground acceleration at zero period. It clearly demonstrates a significant departure from the typical shapes of seismic design spectra, which generally demonstrate substantial attenuation in the long-period range. In addition, like in many other seismic codes, the current Chinese seismic code specifies a maximum period of only 6 s in the design spectrum, which seems inadequate for the seismic design of super tall buildings.

The spectral acceleration at the fundamental periods $S_a(T_1, 5\%)$ of the base motions are summarized in Table 3, along with the peak base acceleration (*PBA*) and peak base velocity (*PBV*), the other two commonly used intensity measures in earthquake engineering. Considering that the primary axes of the building had nothing to do with the direction of the earthquake rupture, the horizontal base motions in the x- and y-direction are first rotated to the direction of maximum acceleration or maximum velocity before calculating *PBA* or *PBV*, respectively. Fig. 7 provides examples of how the maximum acceleration or velocity were determined on the orbits. The $S_a(T_1)$ and the *PBA*s are approximately one to two orders of magnitude smaller than the Chinese code-specified demand at frequency earthquakes (63% in 50 yrs, or 50-yrs return period), which serve as the elastic design limit for seismic analysis.

Fig. 8 summarizes the base motion intensity measures of the four buildings to show their attenuation with respect to the epicentral distances. While the intensity measures of the three buildings of FCT, IFC and JYT attenuated almost linearly with the epicentral distance, the base motion intensities at the CHB in Sanya deviates from the linear regression and were much lower than the others. As shown in Fig. 1, among the four buildings, the CHB was the only one located to the southeast of the epicenter, but the other three have shared similar path of the seismic wave propagation.

5. Engineering demand parameters of the buildings

The peak floor acceleration (*PFA*) and peak inter-story drift ratio (*PIDR*) are the two most commonly-used engineering demand parameters for the rapid damage assessment of buildings subjected to earthquakes. While the *PFA*s of the instrumented floors are readily available from the acceleration readings, the acceleration time histories of the other floors were estimated by linear interpolation of the data of the instrumented floors. For the maximum displacement relative to the base, u_{max}, of all the floors, the linearly interpolated absolute acceleration time-histories of all floors were firstly double integrated into the absolute displacement time-histories, and then subtracted the base motion displacement to give the relative displacement, u, of all the floors above the base. For the *PIDR*s of each story, the absolute acceleration of the lower floor of the story was firstly subtracted from that of the upper floor to give the relative acceleration. It was then double integrated into the

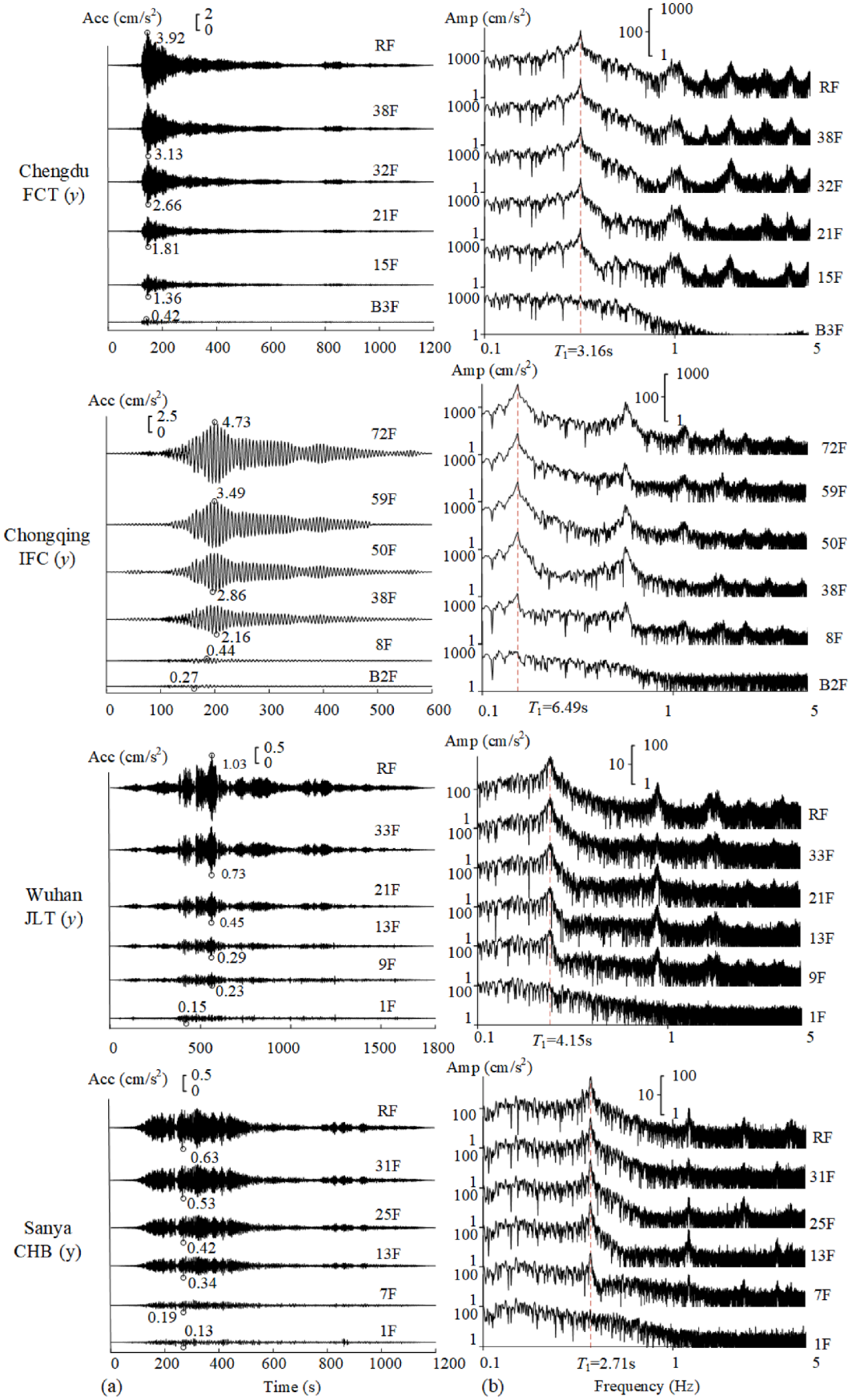

Fig. 3. Acceleration records at selected floors: (a) time histories, (b) Fourier amplitude spectra.

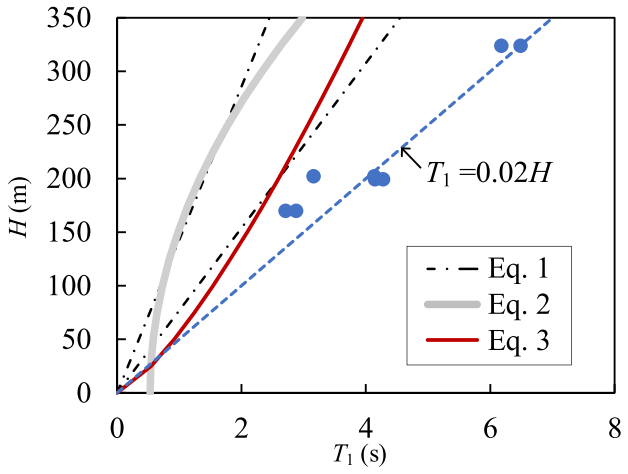

Fig. 4. Relationship of fundamental periods and building height.

relative displacement of the story, which was divided by the story heights to give the inter-story drift ratio. Trapezoidal numerical integration was used to derive velocity from acceleration and displacement from velocity. Before each integration was performed, the data were subjected to (1) baseline correction to remove the mean offset of the records, (2) Hanning window filtering to prevent error accumulation at the beginning and end segments, and (3) non-causal bandpass filtering of 0.1 Hz–20 Hz with a 4th-order Butterworth filter. The results are summarized in Fig. 9.

Despite the significant amplification of floor acceleration along the height, the maximum *PFA*s of all four buildings did not exceed 5 cm/s^2, below which the shaking was hardly perceptible to the occupants in the buildings during the earthquake according to the criteria proposed by Chang (1973). In addition, such small floor accelerations were hardly harmful to any acceleration-sensitive nonstructural elements. Meanwhile, the maximum *PIDR* of the four buildings took place at the top floors of the IFC in Chongqing, which was 0.25%, or 1/4000, far lower than the 1/800 *PIDR* limit specified by the Chinese seismic code (GB 50011-2010, 2016) for RC frame-core tube structures under frequency earthquakes (63% of exceedance in 50 yrs). Such small deformations translated no likely damage to the structural members or displacement-sensitive nonstructural elements.

The height-wise distribution of *PFA*s lays a foundation of determining the seismic demands on nonstructural elements anchored on the floors in the seismic codes such as ASCE 7 in the US (American Society of Civil Engineers, 2022) and GB 50011 in China (GB 50011-2010, 2016), in which a key parameter is the ratio of amplification from bottom to top of a building. Fig. 10(a) summarizes this ratio for the four buildings along its horizontal primary directions during the earthquake, where the ratio is calculated between the peak floor acceleration of the topmost instrumented floor (denoted as *PTA*) and that of the base motion (*PBA*). The ratios varied from 5 to 19. The linear regression of *PBA* and *PTA* suggests a ten-fold amplification of floor acceleration from base to top, which is much larger than the assumed the 2-fold amplification in GB 50011 or the maximum 3.5-fold amplification in ASCE 7.

The Fourier spectra of the records in Fig. 3(b) clearly suggest the dominancy of the 1st mode response. For such a system, the spectral acceleration $S_a(T_1)$ of the base motion is a good estimate for the peak floor acceleration at an equivalent height of the building, which is roughly 2/3 the total height for systems of uniformly distributed stiffness and mass. As shown in Fig. 10(b), the linear regression of the *PBA* and $S_a(T_1)$ of the base motion assuming a 0.5% damping ratio suggests a 6.5-fold amplification of acceleration response. If assuming a linear distribution of *PFA*s, the 6.5 times *PBA* at an equivalent height of 2/3*H* corresponds to a 9.8 times *PBA* at the top, which is very close to the linearly regressed ratios of 10 between the *PBA* and *PTA* in Fig. 10(a). On the other hand, however, if the commonly-used 5% damping ratio is assumed, the ratio is greatly reduced to 3.3 (Fig. 10(c)), much lower than the observation but quite close to the recommended values in the seismic codes. In other words, the 2-fold or 3.5-fold amplifications in the codes may have been established by assuming a 5% damping ratio. If the damping is much lower, which is quite possible as suggested by Cruz and Miranda (2021) and Fan et al. (2025), the simplified equations in the codes may greatly under-estimate the seismic demands on nonstructural elements on the floors. It is also worth noting that an inherent damping ratio of 0.5% has been adopted in the design and consulting practice by institutes like Arup, when the energy dissipation from nonlinearity is explicitly modelled (Huang, 2025).

The measured displacement of the buildings can assist evaluating the overall lateral stiffness of the building under the earthquakes, if com-

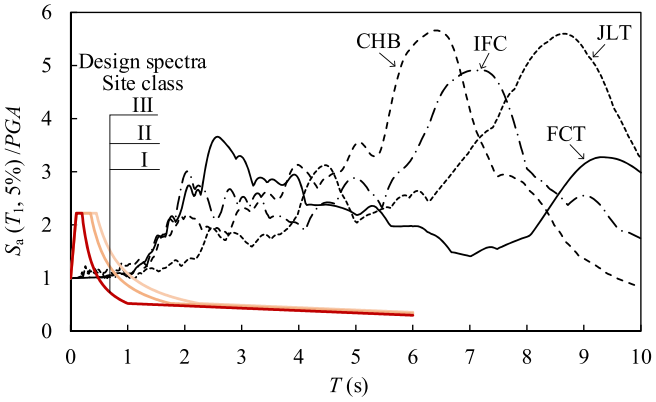

Fig. 6. Comparison of normalized design spectra and recorded response spectra at the bases.

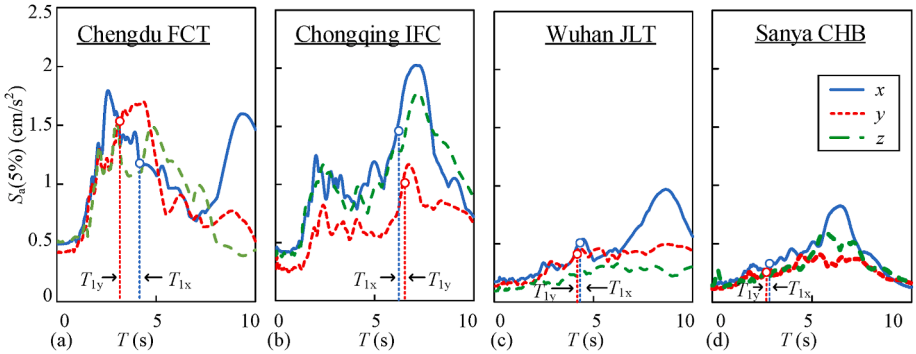

Fig. 5. Acceleration response spectra of base motions (5% damping) of (a) FCT, (b) IFC, (c) JLT, and (d) CHB.

Table 3
Intensity measures of base motions.

Buildings	Assumed base floor	Recorded				Frequent earthquake for seismic design		
		$S_a(T_1, 5\%)$ (cm/s^2)		*PBA* (cm/s^2)	*PBV* (cm/s)	PGA_D (cm/s^2)	$S_{aD}(T_1, 5\%)$ (cm/s^2)	
		x	*y*				*x*	*y*
FCT	B3F	1.17	1.54	0.43	0.29	35	15.33	16.87
IFC	B2F	1.52	1.08	0.38	0.27	18	5.25[a]	5.00[a]
JLT	1F	0.52	0.44	0.16	0.19	18	7.77	7.88
CHB	1F	0.31	0.27	0.11	0.09	18	8.49	8.63

[a] Linearly extrapolated beyond 6s period, which is the code-specified upper limit.

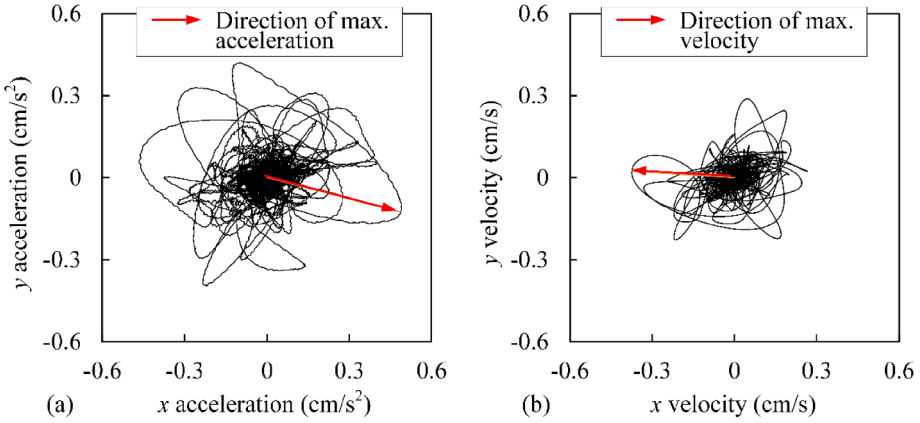

Fig. 7. Orbits of horizontal base motion: (a) acceleration, and (b) velocity.

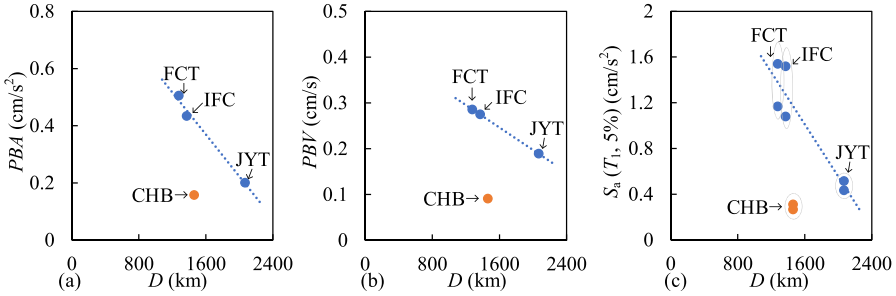

Fig. 8. Attenuation with epicentral distances of (a) *PBA*, (b) *PBV*, and (c) $S_a(T_1,5\%)$.

bined with the excitation intensity at the base. An equivalent stiffness per unit mass $\overline{K}_{eq}$ is defined in Eq. (4) for this purpose, which has a unit of 1/s^2, or equivalently N/m/kg.

$$\overline{K}_{eq} = \frac{IM}{u_{top}} \tag{4}$$

where *IM* is the intensity measure at the base of the building in the unit of acceleration, and u_{top} is the maximum lateral displacement at top the building relative to the base.

Commonly-used acceleration-based *IM*s include the peak acceleration and the spectral acceleration. Both are used to defined the seismic demand in the Chinese seismic provisions for buildings. For sites of the four buildings, the specified *PGA*s and $S_a(T_1, 5\%)$ under frequent earthquakes are referred to the last three columns in Table 4. The corresponding inter-story drift limits θ_{max} for RC frame-core tube structures are defined as a function of the structural height *H* (Eq. (5)) as per the Chinese technical specification for concrete structures of tall buildings (JGJ 3-2010, 2010). The θ_{max} multiplied by the structural height *H* gives a rough estimate of the top displacement u_{top} corresponding to the code-specified drift limit. Combined with the code-specified demands in terms of either PGA_D or S_{aD}, the code-conforming lower bounds of the equivalent stiffness per unit mass can be estimated. They are compared with the $\overline{K}_{eq}$ based on the measured *IM*s and u_{top} in Fig. 11. If the spectral acceleration S_a is used as the *IM*, Fig. 11(a) shows that all the four buildings exhibited much greater lateral stiffness $\overline{K}_{eq}$ than their respective design limits, suggesting a large design margin for seismic drift control. This is quite reasonable because the lateral stiffness is usually dominated by the factors like the wind load or vertical stability, rather than the seismic load. On the other hand, however, if the peak acceleration is used as the *IM*, Fig. 11(b) shows the opposite: the buildings seem to be much more flexible than expected. It only indicates that *PGA* is by no means a suitable *IM* for tall buildings, especially when they are affected by long-period ground motions from distant earthquakes.

$$\theta_{max} = \begin{cases} 1/800, & H \le 150\ \text{m} \\ \text{Linear interpolation}, & 150\ \text{m} < H < 250\ \text{m} \\ 1/500, & H \ge 250\ \text{m} \end{cases} \tag{5}$$

The vibration of tall buildings under long-period ground motions is characterized by very long durations, which may amplify the terror felt

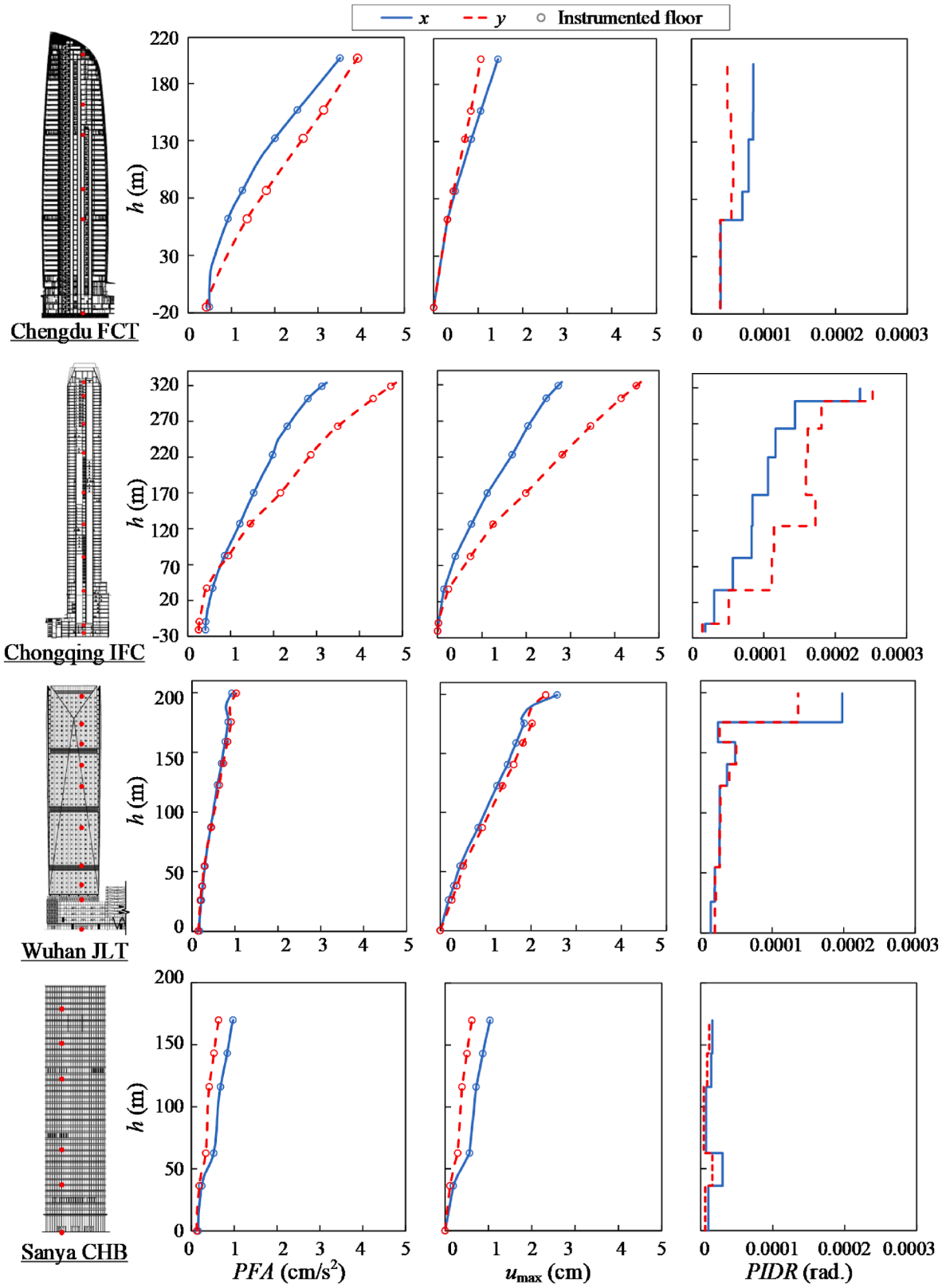

Fig. 9. Height-wise distributions of *PFA*, u_{max}, and *PIDR*.

by people in the buildings. In the Myanmar earthquake whose epicenter was more than 1 000 km away, the vibration at the top of the four tall buildings of concern lasted for 4–13 min in terms of the significant duration $D_{5\text{-}95}$ defined on the normalized Aries intensity (Table 4). However, such long durations seem more a characteristic of the super far-field ground motions rather than the properties of the buildings, because the significant durations of the base motion were comparable to and even larger than those of the motion on top of the buildings (Fig. 12).

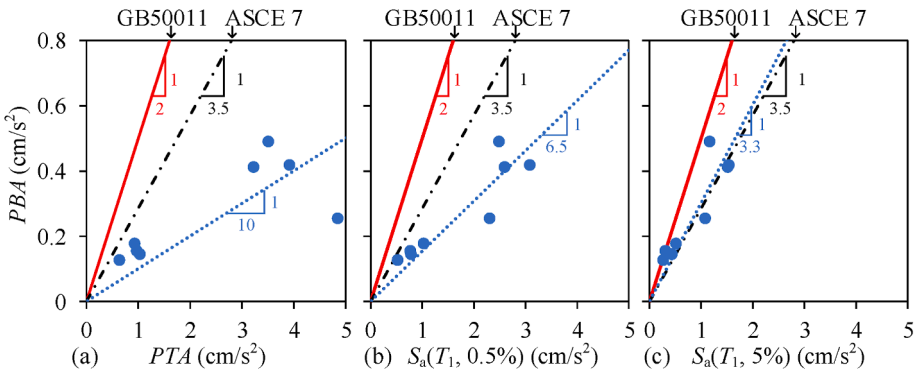

Fig. 10. Amplification of floor acceleration response: (a) recorded peak acceleration at the base and the roof, *PBA* and *PTA*, and relationships of *PBA* and (b) $S_a(T_1, 0.5\%)$, and (c) $S_a(T_1, 0.5\%)$.

Table 4
Significant duration $D_{5\text{-}95}$ of base and top motions (s).

Buildings	Base		Top	
	x	*y*	*x*	*y*
FCT in Chengdu	548.6	489.2	332.3	412.5
IFC in Chongqing	781.7	284.5	225.2	241.6
JLT in Wuhan	664.5	576.1	747.5	789.8
CHB in Sanya	637.5	638.7	432.0	464.6

6. Conclusions

This study presents the recorded responses of four 170 m–320 m tall buildings in southern China to the 2025 M 7.9 Myanmar earthquake at distances of 1 200 km–2 000 km. The engineering demand parameters of *PFA* and *PIDR*s of the buildings' responses were well below the design limits to cause any structural or non-structural damage to the buildings. The following conclusions are drawn from the analyses of the data.

(1) The recorded base motions exhibited significant long-period components in the period range from 2 s to 10 s, which coincides with the fundamental periods of the tall buildings. Both the shape of the response spectra and an analysis of the buildings' lateral stiffness suggest that the peak ground acceleration (*PGA*) is not a suitable intensity measure for tall buildings under remote earthquakes.

(2) The identified fundamental periods of the buildings were 2–3 times larger than the empirical equations in the Chinese design codes. However, the analysis of the equivalent lateral stiffness in terms of the ratio of spectral acceleration and top displacement shows that the buildings were much stiffer than the code requirement to satisfy the drift limit at frequent earthquakes. It suggests that the empirical equations recommended by the Chinese code may be overly conservative.

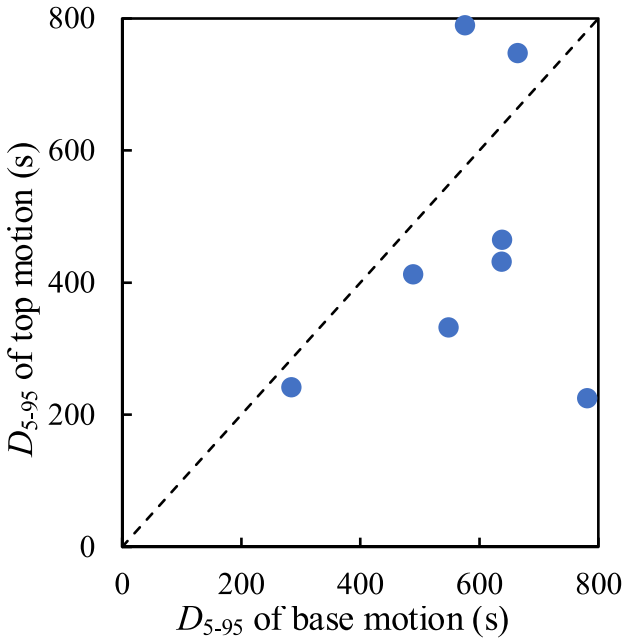

Fig. 12. Significant duration of the base and top motions of the buildings.

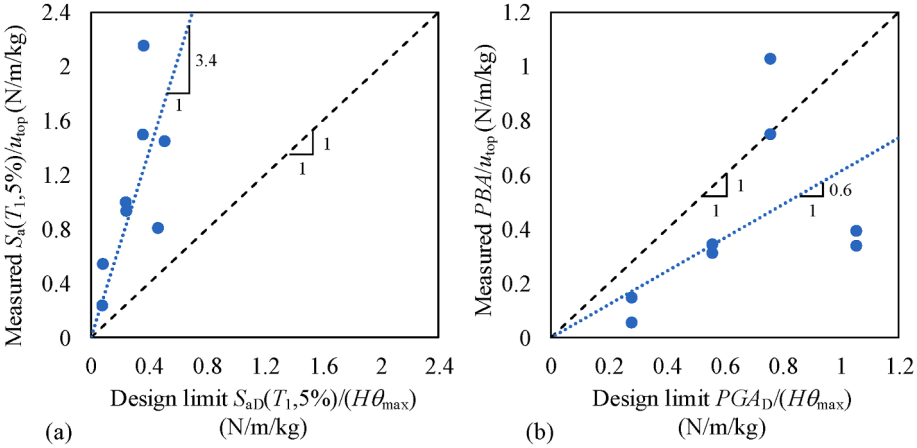

Fig. 11. Equivalent lateral stiffness per unit mass in terms of (a) spectral acceleration, and (b) peak acceleration of base motion.

(3) The horizontal acceleration responses were amplified by 5–19 times from the base to the top of the buildings, significantly exceeding the code-specified values for determining the seismic demands on nonstructural elements. It is possibly attributed to the fact that the seismic code assumes a much larger damping ratio than it actually was for tall buildings.
(4) The vibration of the tall buildings lasted for 4–13 min in terms of the significant durations $D_{5\text{-}95}$, which may amplify the terror felt by people in the buildings. The comparison of the significant durations of the shaking of the base and the upper floors of the buildings shows that the long durations were more a characteristic of the thousands-kilometers long propagation path rather than the properties of the tall buildings.

CRediT authorship contribution statement

Tao Fan: Writing – original draft, Software, Methodology, Investigation, Formal analysis, Data curation, Conceptualization. **Zhe Qu:** Writing – original draft, Supervision, Project administration, Methodology, Investigation, Data curation, Conceptualization. **Jiang Yang:** Resources. **Juan Qin:** Project administration, Formal analysis. **Xiaofeng Xu:** Project administration. **Yuxiu Chen:** Software, Project administration. **Qiong Yuan:** Project administration.

Declaration of competing interest

The authors declare no potential conflicts of interest with respect to the research, authorship, and/or publication of this article. There are no financial or personal relationships with individuals or organizations that could inappropriately influence or bias the content of the manuscript entitled “Recorded Responses of Four Tall Buildings in South China to the M 7.9 Myanmar Earthquake on March 28, 2025”. No competing interests, whether professional or personal, exist regarding any products, services, or companies that might affect the objectivity of the presented research findings or their interpretation. The study was conducted independently without any external influence that could compromise its scientific integrity. The corresponding author Zhe Qu is the deputy editor-in-chief of Earthquake Research Advances and was not involved in the peer review or decision to publish this article.The authors declare the following financial interests/personal relationships which may be considered as potential competing interests: Jiang Yang and Qiong Yuan are currently employed by Wuhan institute of seismology instrument Co.,LTD.

Author agreement and acknowledgment

All authors agree to this publication. The authors are grateful to the Strong Motion Observation Center of the Institute of Engineering Mechanics, China Earthquake Administration, and the Earthquake Agencies of Chongqing, Hubei, and Hainan for promptly sharing the monitoring data following the earthquake. This work is jointly sponsored by the Key Science and Technology Project of the Ministry of Emergency Management of the People’s Republic of China (2024EMST040403), the National Key Research and Development Program of China (2024YFC3012802) and the Scientific Research Fund from Institute of Seismology, CEA and National Institute of Natural Hazards, Ministry of Emergency Management of China (IS202216317). The financial supports are greatly appreciated.

Appendix A. Supplementary data

Supplementary data to this article can be found online at https://doi.org/10.1016/j.eqrea.2025.100395.

References

American Society of Civil Engineers, 2022. Minimum Design Loads and Associated Criteria for Buildings and Other Structures (ASCE/SEI 7-22). https://doi.org/10.1061/9780784415788.
Cai, J., Xi, N., Han, G., Deng, W., Sun, L., 2025. Rapid report of the March 28, 2025 Mw 7.9 Myanmar earthquake. Earthquake Research Advances. https://doi.org/10.1016/j.eqrea.2025.100396.
Carpenter, L.D., Naeim, F., Lew, M., Youssef, N.F., Rojas, F., Saragoni, G.R., Adaros, M.S., 2011. Performance of tall buildings in Santiago, Chile during the 27 February 2010 offshore Maule, Chile earthquake. Struct. Des. Tall Spec. Build. 20 (1), 1–16. https://doi.org/10.1002/tal.667.
Chang, F.K., 1973. Human response to motion in tall buildings. J. Struct. Div. 99 (ST6), 1259–1272.
Cruz, C., Miranda, E., 2021. Damping ratios of the first mode for the seismic analysis of buildings. J. Struct. Eng. 147 (1), 04020300. https://doi.org/10.1061/(ASCE)ST.1943-541X.0002869.
Earthquake Engineering Research Institute, 2010. Learning from Earthquakes: the Mw 8.8 Chile Earthquake of February 27, 2010 [Special report]. https://www.terracon.com/wp-content/uploads/2015/10/Baska2.pdf.
Fan, T., Qu, Z., Yang, J., Liu, X.H., Guo, X.W., 2025. Monitored responses of a high-rise residential building of RC shear wall structure to distance earthquakes. J. Build. Struct. 46 (1), 111–123 (In Chinese).
GB 50009-2012, 2012. Load Code for the Design of Building Structures. China Architecture & Building Press (In Chinese).
GB 50011-2010, 2016. Code for Seismic Design of Buildings. China Architecture & Building Press (In Chinese).
Huang, Y.L., 2025. [Personal Communication].
JGJ 3-2010, 2010. Technical Specification for Concrete Structures of Tall Building. Construction Industry Press (In Chinese).
Kanda, K., Nakashima, M., Suzuki, Y., et al., 2021. “q-NAVI”: a case of market-based implementation of structural health monitoring in Japan. Earthq. Spectra 37 (1), 160–179. https://doi.org/10.1177/8755293020952468.
Kasai, K., Pu, W.C., Wada, A., 2012. Response of passively-controlled tall buildings in Tokyo during 2011 Great East Japan earthquake. In: Proc. 15th WCEE.
Liang, X.W., Dong, Z.P., Wang, Y.S., Deng, M.K., 2009. Damage to tall buildings in areas with large epicentral distance during M8.0 Wenchuan Earthquake. J. Earthq. Eng. Eng. Vib. 29 (1), 24–31 (In Chinese).
Meli, R., Rosenblueth, E., 1986. The 1985 Earthquake causes and effects in Mexico City. Concrete International, ACI, Detroit, Mich 8 (5), 12.
Mizzima News, 2025. Myanmar's Earthquake-Affected Residents Face Insufficient Toilets in Temporary Shelters. April 11, 2025. https://eng.mizzima.com/2025/04/11/21254.
Naeim, F., 1997. Performance of extensively instrumented buildings during the January 17, 1994 Northridge earthquake. An Interactive Information System. Report No. 97, 7530.
Pimanmas, A., 2025. Structural Damages Found in Tall Buildings in Bangkok Form M7.7 Myanmar Earthquake [PowerPoint Presentation]. Webinars on the 2025 Myanmar Earthquake Early Warning System, International Research Institute of Disaster Science. Tohoku University. Retrieved from. https://irides.tohoku.ac.jp/media/files/disaster/eq/myanmar-session_20250425_amorn.pdf.
Saito, T., 2016. Response of high-rise buildings under long period earthquake ground motions. International Journal of Structural and Civil Engineering Research 5 (4), 308–314.
Seed, H.B., Romo, M.P., Sun, J.I., Jaime, A., Lysmer, J., 1988. The Mexico earthquake of September 19, 1985—Relationships between soil conditions and earthquake ground motions. Earthq. Spectra 4 (4), 687–729.
Shi, W., Shan, J., Lu, X., 2012. Modal identification of Shanghai World Financial Center both from free and ambient vibration response. Eng. Struct. 36, 14–26.
Takewaki, I., Murakami, S., Fujita, K., Yoshitomi, S., Tsuji, M., 2011. The 2011 off the Pacific coast of Tohoku earthquake and response of high-rise buildings under long-period ground motions. Soil Dynam. Earthq. Eng. 31 (11), 1511–1528.
The Washington Post, 2025. Damage to Communications and Roads in Myanmar as aid workers assess needs. URL. https://www.washingtonpost.com/world/2025/03/28/myanmar-quake-77-bangkok-thailand/#link-KQARML5TUJHK3NLDEBZYQBIS24. (Accessed 28 March 2025).
U.S. Geological Survey (USGS), 2025. *M* 7.9 Myanmar Earthquake Event Page. URL. https://earthquake.usgs.gov/earthquakes/eventpage/us7000pn9s/executive.